

ISSN 1330-0008

CODEN FIZAE4

INFLUENCE OF THE SUCCESSIVE ANNEALING ON THE  
MAGNETIZATION PROCESSES IN  $\text{Fe}_{73.5}\text{Cu}_1\text{Nb}_3\text{Si}_{15.5}\text{B}_7$  RIBBONSTJEPAN SABOLEK, ŽELJKO MAROHNIĆ<sup>a</sup> and GISELHER HERZER<sup>b</sup>*Department of Physics, Faculty of Science, University of Zagreb, POB 162, Zagreb,  
Croatia*<sup>a</sup>*Institute of Physics of the University, University of Zagreb, POB 304, Zagreb, Croatia*<sup>b</sup>*Vacuumschmelze GmbH, D-63450 Hanau, Germany*

Received 21 November 1996

UDC 538.955

PACS 75.50.Kj, 75.60.-d, 75.60.Ch

The model for the influence of core-current generated field  $H_p$  on the magnetization processes in ferromagnetic ribbons has been employed for the detailed analysis of the  $M - H$  loops and the corresponding  $dM/dt$  vs.  $H$  curves for  $\text{Fe}_{73.5}\text{Cu}_1\text{Nb}_3\text{Si}_{15.5}\text{B}_7$  alloy, successively annealed at different temperatures  $T_a \leq 540$  °C. The analysis shows that in the amorphous state ( $T_a \leq 300$  °C), only fraction of the main (inner) domain structure participates in the process of magnetization. Further annealing strongly reduces the local anisotropy and the average pinning strength of the domain walls  $\langle S_u \rangle$ , which results in a very low coercive field  $H_c$  for  $400$  °C  $\leq T_a \leq 500$  °C. Simultaneously, the maximum magnetization  $M_m$  becomes almost equal to the saturation magnetization  $M_s$  ( $\approx 1.3$  T) already in low magnetizing field ( $H_0 = 100$  A/m). The minimum of  $H_c$  ( $T_a = 450$  °C) is associated with the formation of nanocrystalline  $\text{Fe}_3\text{Si}$  grains, and high  $M_m$  and maximum permeability  $\mu_{max}$  and a low angle  $\langle \delta \rangle$  (between domain magnetizations and the ribbon axis) show that a whole domain structure is very simple in this range of  $T_a$ . Further annealing ( $T_a > 500$  °C) increases  $\langle S_u \rangle$  and  $\langle \delta \rangle$  (which increases  $H_c$ ) and reduces drastically  $\mu_{max}$  which is consistent with the earlier results for similar samples.

## 1. Introduction

Recent investigations have shown that ferromagnetic materials consisting of two different phases, i.e. fine structure of nanocrystalline grains dispersed within the amorphous matrix, may possess exceptionally good soft ferromagnetic properties [1]. Such structures can be obtained by annealing of the amorphous Fe-Cu-Nb-Si-B alloys at suitable temperature [2,3]. In particular, for the  $\text{Fe}_{73.5}\text{Cu}_1\text{Nb}_3\text{Si}_{13.5}\text{B}_9$  alloy, the best properties (very low coercive field  $H_c$  and high initial permeability  $\mu_i$ ) are obtained for the annealing at temperatures  $T_a$  between 500 °C and 550 °C [2,3]. The improvement of the soft magnetic properties is caused by the formation of the fine structure of  $\text{Fe}_3\text{Si}$  nanocrystalline grains (with randomly oriented easy axes of magnetization), dispersed within the amorphous matrix which presents the coupling for the interaction between these grains [2,3]. The magnetocrystalline anisotropy energy  $K$  of  $\text{Fe}_3\text{Si}$  compound is very large ( $K \approx 10^4 \text{ J/m}^3$ ), however, when the grain diameter  $D$  is smaller than the exchange length  $l_k$ , the magnetizations of the particular grains can not follow the direction of the easy axes of the grains because of the exchange interaction between the grains. Therefore, the effective magnetic anisotropy within the sample tends to vanish, which results in extremely soft magnetic properties [2,3].

The investigation of the domain structure and the magnetization processes is particularly important for further improvement of the soft magnetic properties of these materials. Earlier studies have shown that the application of the model for the influence of surface fields  $H_p$  (generated with the direct ( $J_D$ ) or alternating ( $J$ ) core current) on the process of magnetization of amorphous ferromagnetic ribbons [4–7] may provide a good insight into the domain structure, anisotropy and pinning of domain walls (DW) in such samples [8,9]. In particular, the analysis of the influence of  $H_p$  on the  $M - H$  loops and the  $dM/dt$  vs.  $H$  curves allows to estimate the average angle  $\langle \delta \rangle$  between the magnetizations ( $I$ ) of the individual groups of domains (which contribute to magnetization of the sample) and the ribbon axis, and of the average pinning strength  $\langle S_u \rangle$  of the corresponding DWs [8]. It is particularly important that in this simple manner one can gain an insight into the main (inner) domain structure (MDS) and the relevant magnetization mechanisms. Such investigations of the  $\text{Fe}_{73.5}\text{Cu}_1\text{Nb}_3\text{Si}_{15.5}\text{B}_7$  ribbon (hereafter FeCuNbSiB) in the amorphous state [10] have shown that its very bad soft magnetic properties (high  $H_c$ , low maximum magnetization  $M_m$ , all in relatively low magnetizing fields,  $H_0 \leq 300 \text{ A/m}$ ) are associated with very strong local anisotropy which is probably due to internal stresses, structural defects and inhomogeneities in these samples [11].

Here we use the analysis of the  $M - H$  loops (obtained with and without core currents  $J$  and  $J_D$ ) for the discussion of the changes in the domain structure, DW pinning and the magnetization mechanisms of FeCuNbSiB sample during the successive annealing at different temperatures  $T_a$ . We also consider some possibilities for the further decrease of  $H_c$  and loss  $E$  in these materials in the nanocrystalline state.

## 2. Experimental techniques

The FeCuNbSiB sample, in the form of a long thin ribbon of dimensions  $l \times w \times t = 200 \text{ mm} \times 2 \text{ mm} \times 0.025 \text{ mm}$ , was prepared with a melt-spinning technique at the Vacuumschmelze GmbH, Hanau. The magnetization measurements were performed with an induction technique at room temperature [12]. The magnetizing field  $H(t)$  of triangular form with the amplitude  $H_0 = 100 \text{ A/m}$  was used for most of the measurements. The exception were the measurements of the dependence of  $H_c$  and remanent magnetization  $M_r$  on  $M_m$  in which the measurements were performed for different values of  $H_0$ . In all measurements, the frequency ( $f$ ) of the drive field was 5.5 Hz. During the magnetization process, a direct ( $J_D$ ) or an alternating current  $J = J_0 \sin \omega t$ , with preselected amplitude, was flowing along the ribbon.  $J$  was suitably synchronized with  $H$  [7]. For the application of core currents, the sample was supplied with the Pt current leads, spot-welded at the ends of the ribbon. In order to enable the annealing and yet to have the sample in fixed position, the sample was inserted into a thin quartz tube (inner diameter close to the width  $w$  of the sample) and fixed into straight position via the Pt current leads.

TABLE 1.

Data relevant to  $\text{Fe}_{73.5}\text{Cu}_1\text{Nb}_3\text{Si}_{15.5}\text{B}_7$  sample:  $T_a$  is the annealing temperature;  $H_c$ ,  $M_r$ ,  $M_m$  and  $\mu_{max}$  are the coercive field, remanent magnetization, maximum magnetization and maximum permeability, respectively, determined from the  $M - H$  loops;  $\langle \delta \rangle$  (DC) and  $\langle \delta \rangle$  (AC) are the average angles between the magnetization of the domains ( $I$ ) and the ribbon axis deduced from the variations of positions ( $C$ ) of the center of the  $M - H$  loops and  $H_c$  with  $H_p(J_D)$  and  $H_{p0}(J)$ , respectively;  $\langle S_u \rangle$  is the average strength of pinning of domain walls. Triangular drive field with the amplitude  $H_0 = 100 \text{ A/m}$  and frequency  $f = 5.5 \text{ Hz}$  was used.

$T_a$ (°C)	$H_c$ (A/m)	$\langle S_u \rangle$ (A/m)	$M_r$ (T)	$M_m$ (T)	$\mu_{max}$ ( $10^4 \text{ Tm/A}$ )	$\langle \delta \rangle$ (DC)	$\langle \delta \rangle$ (AC)
prean.	13.5	13.5	0.31	0.49	7.4	3°	4°
200	12.4	12.4	0.29	0.49	6.6	2°	3°
300	8.2	8.2	0.30	0.66	6.5	4°	7°
400	2.5	2.5	0.33	1.26	9.1	1°	1°
450	2.1	2.1	0.23	1.29	9.2	6°	5°
500	2.9	2.9	0.29	1.26	8.2	7°	4°
540	6.5	6.0	0.33	1.21	6.5	24°	22°

The measurements of the  $M - H$  loops and  $dM/dt$  vs.  $H$  curves were first performed on as-quenched (amorphous) sample and then repeated after each (successive) annealing step. The annealing temperatures  $T_a$  are given in Table 1. The annealing was performed in the flowing argon atmosphere in the long horizontal furnace. The sample was first heated up to  $T_a$  (with the average heating rate of about 15 K/min.), kept for one hour at  $T_a$ , furnace cooled to 200 °C (average

cooling rate about 3 K/min.) and than removed from the furnace (rapid cooling to room temperature).

In order to get an insight into the microstructure of annealed samples we have annealed a reference sample together with the measured one at  $T_a = 450$  °C, 500 °C and 540 °C. The X-ray diffraction pattern of the reference sample (taken after last anneal at 540 °C) has shown peaks corresponding to nanocrystalline phase composed of Fe<sub>3</sub>Si grains only. The average diameter  $D$  of these grains was calculated by the use of relation  $D = 0.9\lambda/(\beta_{1/2} \cos \theta)$ , where  $\lambda = 1.5418 \times 10^{-10}$  m is the wavelength of the employed X-rays,  $\beta_{1/2}$  is the width of the diffraction peak at half of its maximum and  $\theta$  is the Bragg's diffraction angle. We employed two peaks and obtained very similar values for  $D$  ( $D = 12$  nm and 14 nm, respectively).

The measurements of the initial AC susceptibility has been used in order to determine the magnetic properties (the Curie temperature  $T_c$ ) of the as-quenched (amorphous) sample and that annealed at 540 °C. For this purpose, small pieces ( $\leq 20$  mm in length) were cut from the ribbons already used for the measurements of the  $M - H$  loops and measured with the standard AC susceptibility technique.

### 3. Results and discussion

The influence of successive annealing on the process of magnetization of FeCuNbSiB sample is illustrated in Fig. 1. Here, the  $M - H$  loops and the corresponding  $dM/dH$  vs.  $H$  curves for the as-quenched sample and those after its annealing at  $T_a = 450$  °C and 540 °C are shown. We note very different shapes of these curves. From the  $M - H$  loops, similar to those depicted in Fig. 1, we have determined the coercive field  $H_c$ , the maximum magnetization  $M_m$ , the remanent magnetization  $M_r$  and the maximum permeability  $\mu_{max}$  at all annealing temperatures  $T_a$  (Table 1). The variations of these parameters with  $T_a$  are shown in Figs. 2 and 3. In order to obtain an insight into the changes in the domain structure (which contributes to magnetization for given  $H_0$ ) and pinning of the corresponding domain walls (DW), we have investigated the effects of the direct ( $J_D$ ) and alternating ( $J$ ) core currents (i.e. of the associated surface fields  $H_p = J_D/2w$ , where  $w$  is the width of the ribbon) on the  $M - H$  loops after each annealing step. In particular, according to the model for the influence of  $H_p$  generated by  $J_D$  on the process of magnetization of long and thin amorphous ferromagnetic ribbons,  $J_D$  can cause a shift of the  $M - H$  loop [4-6]. The position  $C$  of the center of the  $M - H$  loop is than given by [4-6]:

$$C = \pm H_p \tan \langle \delta \rangle . \quad (1)$$

Here  $\langle \delta \rangle$  is the average angle between the magnetizations  $I$  of the domains contributing to magnetization and the ribbon axis and different signs correspond to different directions of  $J_D$ . The same model also predicts that an alternating core current  $J = J_0 \sin \omega t$  (suitably synchronized with the magnetizing field  $H$  [6])

causes the reduction of  $H_c$  [6,7]:

$$H_c = H_{c0} - H_{p0} \tan \langle \delta \rangle, \quad (2)$$

where  $H_{c0}$  is the coercive field in the absence of core current and  $H_{p0} = J_0/2w$ . Relations (1) and (2) were used in order to deduce  $\langle \delta \rangle$  for different  $T_a$  from the variations  $C$  and  $H_c$  with  $H_p$  and  $H_{p0}$ , respectively. The knowledge of  $\langle \delta \rangle$  can be used to estimate the average strength of pinning of DWs which contribute to magnetization along the ribbon axis [8,9]:

$$\langle S_u \rangle = H_{c0} \cos \langle \delta \rangle. \quad (3)$$

The knowledge of both  $\langle S_u \rangle$  and  $\langle \delta \rangle$  can provide a good insight into the local anisotropy and the MDS, which participates in the process of magnetization for a given amplitude  $H_0$  of the magnetizing field  $H$  [8,13].

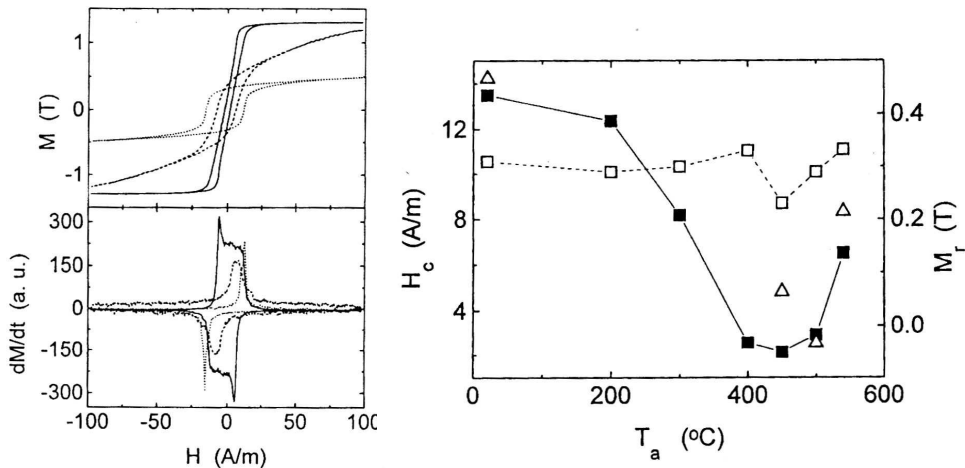


Fig. 1.  $M - H$  loops (a) and the corresponding  $dM/dt$  vs.  $H$  curves (b) for  $\text{Fe}_{73.5}\text{Cu}_1\text{Nb}_3\text{Si}_{15.5}\text{B}_7$  sample before annealing ( $\cdot \cdot \cdot$ ) and after annealing at  $T_a = 450^\circ\text{C}$  ( $-$ ) and  $540^\circ\text{C}$  ( $- - -$ ). The measurements were performed using triangular drive field with the amplitude  $H_0 = 100$  A/m and frequency  $f = 5.5$  Hz.

Fig. 2. Variation of the coercive field  $H_c$  (□) and the remanent magnetization  $M_r$  (□) with the annealing temperature  $T_a$  for the  $\text{Fe}_{73.5}\text{Cu}_1\text{Nb}_3\text{Si}_{15.5}\text{B}_7$  sample. Symbols  $\Delta$  show the variation of  $H_c$  with  $T_a$  for the reference sample (see text). The same conditions of measurements as in Fig. 1 were used (right).

From Fig. 1 and the data in Table 1, it is clear that the as-quenched (amorphous)  $\text{FeCuNbSiB}$  sample has very bad soft magnetic properties (i.e. large  $H_c = 13.5$  A/m and low  $M_m \approx 0.35M_s$  for  $H_0 = 100$  A/m). Low  $M_m$  and  $\langle \delta \rangle \approx 3^\circ$  (Table 1 and inset in Fig. 3) show that only a fraction of MDS with magnetizations  $I$  approximately parallel to ribbon axis participates in the process

of magnetization of amorphous FeCuNbSiB sample for  $H_0 = 100$  A/m. Since in the amorphous sample in this range of  $H_0$  the irreversible motion of DWs dominates the magnetization process [2], we conclude that a very strong local anisotropy forms strong volume pinning centres [11] within the sample which for given  $H_0$  prevent the motion of DWs for a sizable fraction ( $\approx 50\%$ ) of MDS. (The existence of a strong local anisotropy in the as-quenched samples was confirmed in the recent investigation of the influence of the torsion and tensile stress on the magnetization of as-quenched FeCuNbSiB samples [10].) Furthermore, the dependence of  $H_c$  on  $M_m/M_s$  (Fig. 4) shows that a single type of pinning centres determines the motion of DWs responsible for the magnetization of amorphous FeCuNbSiB samples (the slope of  $\log H_c$  vs.  $\log M_m/M_s$  variation is approximately constant within the explored range of  $M_m/M_s$ ) [14]. However,  $M_r$  tends to saturate for  $M_m/M_s > 0.4$  (Fig. 5) in spite of the increase of  $H_c$  with  $M_m/M_s$  in the same range of  $M_m$  (Fig. 4). This seems to indicate that the process of magnetization for  $M_m/M_s > 0.4$  involves the bulging of the parts of DWs pinned between the strong pinning centres [14].

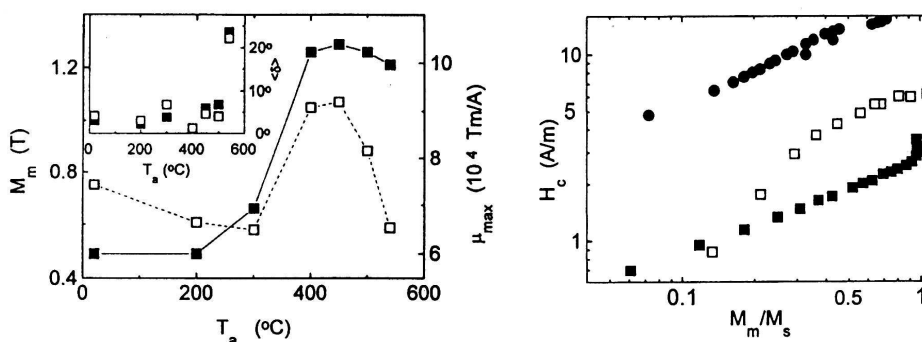


Fig. 3. Variation of maximum magnetization  $M_m$  ( $\blacksquare$ ) and the maximum permeability  $\mu_{max}$  ( $\square$ ) with the annealing temperature  $T_a$  for the  $\text{Fe}_{73.5}\text{Cu}_1\text{Nb}_3\text{Si}_{15.5}\text{B}_7$  sample. The conditions of measurements were otherwise the same as in Fig. 1. Inset: the dependence of the average angle  $\langle \delta \rangle$  between the domain magnetizations and the ribbon axis on the annealing temperature  $T_a$  for the  $\text{Fe}_{73.5}\text{Cu}_1\text{Nb}_3\text{Si}_{15.5}\text{B}_7$  sample. The symbols  $\square$  and  $\square$  denote  $\langle \delta \rangle$  determined for the direct ( $\langle \delta \rangle$ (DC) in Table 1) and alternating core current ( $\langle \delta \rangle$ (AC) in Table 1), respectively.

Fig. 4. Variation of the coercive field  $H_c$  with the normalized magnetization  $M_m/M_s$  for the  $\text{Fe}_{73.5}\text{Cu}_1\text{Nb}_3\text{Si}_{15.5}\text{B}_7$  sample in the as-quenched state ( $\circ$ ) and after annealing at  $T_a = 500$  °C ( $\square$ ) and  $540$  °C ( $\square$ ). The frequency of the drive field was  $5.5$  Hz (right).

During the annealing up to  $T_a = 300$  °C,  $H_c$  decreases quite rapidly with  $T_a$  (Fig. 2), whereas  $M_m$  increases quite slowly with  $T_a$  (Fig. 3). In the same range of  $T_a$ ,  $M_r$  is approximately constant (Fig. 2) and  $\mu_{max}$  decreases with  $T_a$  (Fig. 3). Since the angle  $\langle \delta \rangle$  varies rather little around  $4^\circ$  (inset in Fig. 3) in this range of  $T_a$ , it seems that the main reason for decrease of  $H_c$  is the reduction of the average pinning strength  $\langle S_u \rangle$  of DWs (Table 1). For  $T_a \leq 300$  °C  $\langle S_u \rangle$  most probably

decreases (Table 1) due to the reduction in the local anisotropy associated with the annealing out of the internal stresses and local defects (formed during the sample preparation) [15]. Due to the decrease in the local anisotropy, the same domains from MDS which did not participate earlier in the process of magnetization along the ribbon axis do so after annealing at 300 °C. Their participation is made visible through the simultaneous increase of the angle  $\langle \delta \rangle$  (inset in Fig. 3) and  $M_m$  (Fig. 3) at  $T_a = 300$  °C. Simultaneously, the participation of domains with different angles  $\delta$  in the process of magnetization decreases  $\mu_{max}$ , as observed in Fig. 3 for  $T_a \leq 300$  °C.

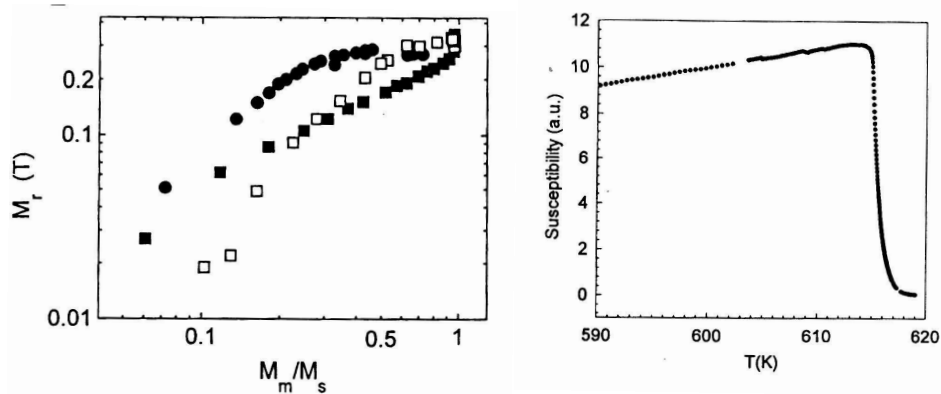


Fig. 5. Variation of the remanent magnetization  $M_r$  with the normalized magnetization  $M_m/M_s$  for the  $Fe_{73.5}Cu_1Nb_3Si_{15.5}B_7$  sample in the as-quenched state ( $\circ$ ) and after annealing at  $T_a = 500$  °C ( $\square$ ) and  $540$  °C ( $\square$ ). The frequency of the drive field was 5.5 Hz.

Fig. 6. Variation of the initial susceptibility with the temperature  $T$  for the  $Fe_{73.5}Cu_1Nb_3Si_{15.5}B_7$  sample in the as-quenched state (right).

After annealing at  $T_a = 400$  °C,  $H_c$  falls suddenly to 2.5 A/m (Fig. 2 and Table 1), whereas  $M_m$  increases to a value close to  $M_s$  (Fig. 3). Also  $\mu_{max}$  suddenly increases at  $T_a = 400$  °C (Fig. 3). Figures 2 and 3 show that our sample shows the best soft magnetic properties after annealing at temperatures between 400 °C and 500 °C. In this range of  $T_a$ ,  $H_c$  has the lowest magnitudes (the minimum  $H_c \approx 2$  A/m is reached for  $T_a = 450$  °C), which means that already the annealing at 400 °C lead to the formation of nanocrystalline  $Fe_3Si$  grains [2,3]. The observed variation of  $H_c$  with  $T_a$  (Fig. 2) is similar to that observed by other authors [2,3], however, due to the prolonged stay of the sample in the furnace (the periods of heating up to  $T_a$  and cooling down to 200 °C), the formation of the nanocrystalline phase occurred at somewhat lower temperatures  $T_a$  than those reported in the literature [2,3]. In particular, the minimum of  $H_c$  is reached at  $T_a$  which is some 50 – 90 °C lower than those observed by the other authors [2,3]. The above conclusion is supported by the measurements for the reference sample which was annealed at  $T_a = 450$  °C, 500 °C and 540 °C only. For this sample,  $H_c$  reaches minimum at

$T_a = 500$  °C (Fig. 3), i.e. at  $T_a$  which is 50 °C higher than that for the sample which spent more time in the furnace. Furthermore, the analysis of the X-ray diffraction patterns for the reference sample (obtained after the anneal at 540 °C) showed the existence of the nanocrystalline grains with the diameters 12 – 14 nm. The measurements of the Curie temperatures  $T_c$  for the amorphous sample and sample annealed at 540 °C also showed the existence of the nanocrystalline phase in the annealed one. As shown in Fig. 6, the amorphous sample exhibits rather sharp transition at  $T_c \approx 342$  °C, whereas the sample annealed at 540 °C shows very sharp transition with  $T_c \approx 569$  °C (Fig. 7), which corresponds to that of the nanocrystalline Fe–Si grains. Our results for  $T_c$ 's agree rather well with those of other authors for similar alloys [2,3]. Figure 7 also shows the change in the slope of the initial susceptibility for the annealed sample around 290 °C which probably corresponds to a smeared ferromagnetic transition of the residual amorphous phase. However, since at this stage of annealing the nanocrystalline phase should be the dominant one (about 80% of volume [3]) and the residual (minority) amorphous phase is rather inhomogeneous (concentration fluctuations), its transition (smeared over a sizable temperature range) does not have drastic effect on the susceptibility variation of the annealed sample. Sizable lower average  $T_c$  of the residual amorphous phase, compared to that of the as-quenched amorphous sample ( $T_c = 342$  °C), is due to change in the composition of amorphous phase after separation of Fe–Si grains (the enrichment in Nb and B and decrease in Fe content).

Upon the formation of the fine structure of  $\text{Fe}_3\text{Si}$  nanocrystalline grains ( $400$  °C  $\leq T_a \leq 500$  °C), the local anisotropy vanishes [2,3], which explains the drastic reduction of  $H_c$  and sharp increase of  $M_m$ . Very high  $M_m$  in this range of  $T_a$  (for  $T_a = 450$  °C,  $M_m \approx M_s$ ) shows that practically whole domain structure of the sample participates in the process of magnetization. The analysis of the influence of  $J_D$  and  $J$  on  $C$  and  $H_c$  (Eqs. (1) and (2)) shows that  $\langle \delta \rangle \approx 4^\circ$  remains quite small (inset in Fig. 3 and Table 1) for  $400$  °C  $\leq T_a \leq 500$  °C. Rather low  $\langle \delta \rangle$  and large  $M_m$  and  $\mu_{max}$  indicate quite simple domain structure in this range of  $T_a$ . The entire domain system seems to consist of domains with magnetizations nearly parallel to the ribbon axis, and the magnetization occurs through the motion of their DWs. The volume pinning of DWs vanishes with the disappearance of the local anisotropy within the sample, and the main DW pinning centres for  $400$  °C  $\leq T_a \leq 500$  °C are the surface defects and irregularities. The variation of  $H_c$  with  $M_m/M_s$  for  $T_a = 500$  °C, showing two distinctly different regions of the increase of  $H_c$  with  $M_m/M_s$  (Fig. 4), confirms this conclusion. These two regimes are thought to correspond to two different types of the pinning centres, possessing different strengths [14] (the steeper increase of  $H_c$  at elevated  $M_m$  corresponds to stronger pinning centres). Therefore, the pinning mechanism of DWs in FeCuNbSiB sample for  $400$  °C  $\leq T_a \leq 500$  °C is similar to that observed in the nonmagnetostrictive Co-based amorphous ferromagnets [14]. As seen from Fig. 5, for  $T_a = 500$  °C,  $M_r$  shows the same dependence on  $M_m/M_s$  as  $H_c$ . This shows that in this range of  $T_a$  even the strongest pinning centres are sufficiently weak, which allows that magnetization up to practically  $M_s$  occurs via the irreversible motion of DWs.



After the annealing at  $T_a = 540$  °C,  $H_c$  suddenly increases (Fig. 2 and Table 1). Figure 2 and inset in Fig. 3 show that both  $\langle \delta \rangle$  and  $\langle S_u \rangle$  participate in the increase of  $H_c$ . This increase of  $H_c$  is most probably associated with the appearance of the uniaxial anisotropy (similar to that induced by torsion in the magnetostrictive amorphous alloys [9,16]), which may arise from the local stresses and/or increased size of the nanocrystalline grains ( $D \approx 14$  nm) due to annealing at elevated  $T_a$ . The appearance of the anisotropy affects the domain structure [2] and is also confirmed by the rapid decrease of  $\mu_{max}$ , which starts already for  $T_a > 450$  °C (Fig. 3). The shape of the  $M - H$  loop for  $T_a = 540$  °C (Fig. 1) shows that at lower  $H \leq 25$  A/m (i.e. up to  $M_m \approx 0.6M_s$ ), the magnetization occurs via irreversible motion of DWs, whereas at higher  $H$  the reversible rotation processes seem to dominate. The variation of  $H_c$  with  $M_m/M_s$  for  $T_a = 540$  °C (Fig. 4) confirms these conclusions.  $H_c$  increases with  $M_m/M_s$  to about  $M_m/M_s \approx 0.6$  (irreversible motion of DWs), but saturates at larger  $M_m$  (reversible rotation processes).  $M_r$  shows similar variation with  $M_m/M_s$  (Fig. 5) as  $H_c$ , which supports the above conclusions about the magnetization processes for  $T_a = 540$  °C.

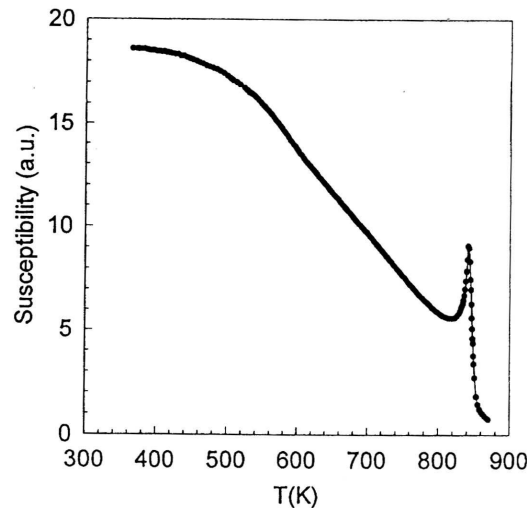


Fig. 7. Variation of the initial susceptibility with the temperature  $T$  for the  $\text{Fe}_{73.5}\text{Cu}_1\text{Nb}_3\text{Si}_{15.5}\text{B}_7$  sample after annealing at  $T_a = 540$  °C.

#### 4. Conclusion

Our results for the changes of the coercive field  $H_c$ , remanent magnetization  $M_r$ , maximum magnetization  $M_m$  and maximum permeability  $\mu_{max}$  with the annealing temperature  $T_a$  for  $\text{Fe}_{73.5}\text{Cu}_1\text{Nb}_3\text{Si}_{15.5}\text{B}_7$  alloy agree well with those obtained for similar  $\text{FeCuNbSiB}$  alloys [2,3]. The presented analysis of the  $M - H$  loops and their changes under the influence of the core currents provides good insight into the domain structure and magnetization processes at different stages of annealing.

Strong volume pinning of domain walls ( $\langle S_u \rangle \approx H_c$ ), which exist in the sample

in the as-quenched (amorphous) state, decreases initially with  $T_a$  ( $T_a \leq 300$  °C) due to reduction of the local magnetic anisotropy. This anisotropy vanishes upon the formation of the nanocrystalline structure ( $400$  °C  $\leq T_a \leq 500$  °C), which results in a minimum of  $\langle S_u \rangle$  and  $H_c$  and maximum of  $M_m$  ( $\approx M_s$ ). In this range of  $T_a$ , low  $\langle S_u \rangle$  and angle  $\langle \delta \rangle$ , high  $M_m$  and Z-shape of the  $M-H$  loop show that the entire domain structure is rather simple (the magnetizations of the domains are nearly parallel to the ribbon axis) and the dependence of  $H_c$  on  $M_m/M_s$  shows that the mechanism of pinning of DWs (surface pinning) is similar to that observed in Co-base nonmagnetostrictive amorphous ferromagnets. Because of this, we conclude that the soft magnetic properties of the nanocrystalline ferromagnetic alloys (especially  $H_c$ ) can be further improved by eliminating the surface pinning via polishing of the surface, or with some other treatment, which will be studied in our future work.

#### Acknowledgement

We wish to thank Dr. S. Popović for the X-ray study of the reference sample. Miss. O. Jovanović helped us with the measurements.

#### References

- 1) Y. Yoshizawa and K. Yamauchi, IEEE Trans. Magnetics **25** (1989) 3324;
- 2) B. Hofman, T. Reininger and H. Kronmüller, Phys. Stat. Sol.(a) **134** (1992) 247;
- 3) G. Herzer, Physica Scripta T **49** (1993) 307;
- 4) J. Horvat, Phys. Stat. Sol. (a) **129** (1992) 519;
- 5) S. Sabolek, E. Babić and K Zadro, Fizika A1 (1992) 167;
- 6) S. Sabolek, IEEE Trans. Magnetics **30** (1994) 919;
- 7) S. Sabolek, E. Babić and Ž. Marohnić, Phys. Rev. B **48** (1993) 6206;
- 8) S. Sabolek, E. Babić and M. Šušak, J. Magnetism magnetic Mater. **149** (1995) 331;
- 9) S. Sabolek, Lj. Erceg and E. Babić, Phys. Stat. Sol. (a) **148** (1995) 283;
- 10) S. Sabolek, E. Babić and Lj. Erceg, J. Magnetism magnetic Mater., to be published;
- 11) H. Kronmüller, J. Magnetism magnetic Mater. **24** (1981) 159;
- 12) J. Horvat, Ž. Marohnić and E. Babić, J. Magnetism magnetic Mater. **82** (1989) 5;
- 13) P. Schönhuber, H. Pfützner, G. Harasko, T. Klinger and K. Futschik, J. Magnetism magnetic Mater. **112** (1992) 349;
- 14) J. Horvat, E. Babić, Ž. Marohnić and H. H. Liebermann, J. Magnetism magnetic Mater. **87** (1990) 339;
- 15) F. E. Luborsky, J. J. Beker and R. O. McCary, IEEE Trans. Magnetics MAG-**11** (1975) 1644;
- 16) J. M. Barandiaran, A. Hernando and E. Ascasibar, J. Phys. D **12** (1979) 1943;
- 17) F. Bodker, S. Morup and S. Linderth, Phys. Rev. Lett **72** (1994) 282.

UTJECAJ UZASTOPNOG NAPUŠTANJA NA PROCESSE  
MAGNETIZIRANJA  $\text{Fe}_{73.5}\text{Cu}_1\text{Nb}_3\text{Si}_{15.5}\text{B}_7$  VRPCE

Model za utjecaj polja  $H_p$ , generiranih strujom kroz uzorak, na procese magnetiziranja u feromagnetskim vrpčama iskorišten je za detaljne analize  $M - H$  krivulja i odgovarajućih ovisnosti  $dM/dt$  o  $H$  krivuljama uzastopno napuštane  $\text{Fe}_{73.5}\text{Cu}_1\text{Nb}_3\text{Si}_{15.5}\text{B}_7$  vrpce na različitim temperaturama ( $T_a \leq 540$  °C). Analize pokazuju da u amorfnom stanju ( $T_a \leq 300$  °C) samo dio glavne domenske strukture sudjeluje u procesu magnetiziranja. Napuštanjem na višim temperaturama naglo se smanjuje lokalna anizotropija i srednja jakost zapinjanja domenskih zidova  $\langle S_u \rangle$ . To rezultira vrlo niskim koercitivnim poljem  $H_c$  za  $400$  °C  $\leq T_a \leq 500$  °C. Istovremeno, maksimalna magnetizacija  $M_m$  postaje približno jednaka magnetizaciji saturacije  $M_s$  ( $\approx 1.3$  T) u niskom magnetizirajućem polju ( $H_0 = 100$  A/m). Minimum  $H_c$  ( $T_a = 450$  °C) je povezan sa stvaranjem nanokristalnih  $\text{Fe}_3\text{Si}$  zrna, a visoka  $M_m$  i maksimalna permeabilnost  $\mu_{max}$  te mali kut  $\langle \delta \rangle$  (između magnetizacija domena i osi vrpce) pokazuju da je cjelokupna domenska struktura vrlo jednostavna u tom području  $T_a$ . Napuštanje na višim temperaturama ( $T_a > 500$  °C) izaziva porast  $\langle S_u \rangle$  i  $\langle \delta \rangle$  (zbog čega raste i  $H_c$ ) te nagli pad  $\mu_{max}$  što je u skladu s drugim rezultatima za slične uzorke.